

Research Article

Bilberry and its main constituents have neuroprotective effects against retinal neuronal damage *in vitro* and *in vivo*

Nozomu Matsunaga¹, Shunsuke Imai¹, Yuta Inokuchi¹, Masamitsu Shimazawa¹, Shigeru Yokota², Yoko Araki³ and Hideaki Hara¹

¹ Department of Biofunctional Evaluation, Molecular Pharmacology, Gifu Pharmaceutical University, Gifu, Japan

² Wakasa Seikatsu Co. Ltd., Kyoto, Japan

³ API Co. Ltd., Gifu, Japan

Our aim was to determine whether a *Vaccinium myrtillus* (bilberry) anthocyanoside (VMA) and/or its main anthocyanidin constituents (cyanidin, delphinidin, and malvidin) can protect retinal ganglion cells (RGCs) against retinal damage *in vitro* and *in vivo*. In RGC cultures (RGC-5, a rat ganglion cell-line transformed using E1A virus) *in vitro*, cell damage and radical activation were induced by 3-(4-morpholinyl) sydnonimine hydrochloride (SIN-1, a peroxynitrite donor). Cell viability was measured using a water-soluble tetrazolium salt assay. Intracellular radical activation within RGC-5 cells was evaluated using 5-(and-6)-chloromethyl-2,7-dichlorodihydrofluorescein diacetate acetyl ester (CM-H₂DCFDA). Lipid peroxidation was assessed using the supernatant fraction of mouse forebrain homogenates. In mice *in vivo*, we evaluated the effects of VMA on *N*-methyl-D-aspartic acid (NMDA)-induced retinal damage using hematoxylin-eosin and terminal deoxynucleotidyl transferase-mediated dUTP nick-end labeling (TUNEL) stainings. VMA and all three anthocyanidins (i) significantly inhibited SIN-1-induced neurotoxicity and radical activation in RGC-5, (ii) concentration-dependently inhibited lipid peroxidation in mouse forebrain homogenates. Intravitreally injected VMA significantly inhibited the NMDA-induced morphological retinal damage and increase in TUNEL-positive cells in the ganglion cell layer. Thus, VMA and its anthocyanidins have neuroprotective effects (exerted at least in part *via* an anti-oxidation mechanism) in these *in vitro* and *in vivo* models of retinal diseases.

Keywords: Lipid peroxidation / NMDA / Oxidative stress / Retinal ganglion cell / SIN-1

Received: August 27, 2008; revised: October 10, 2008; accepted: October 18, 2008

1 Introduction

Retinal ganglion cell (RGC) death is a common feature of many opthalmic disorders such as glaucoma, optic neuro-

pathies, diabetic retinopathy, and retinal vein occlusions. RGC death may occur via a variety of mechanisms involving oxidative stress [1], excitatory amino acids [2], nitric oxide [3], lipid peroxidation [4], apoptosis [5], and/or ER stress [6].

Vaccinium myrtillus (bilberry), a member of the ericaceous family, grows in the mountains and forests of Europe and North America. *V. myrtillus* extracts containing 15 different anthocyanins [7, 8] have been shown to possess potent antioxidant properties [8, 9], and to stabilize collagen fibers [10], promote collagen biosynthesis [10], inhibit platelet aggregation [11], and reduce angiogenesis [12]. Animal studies have demonstrated *V. myrtillus* anthocyanoside (VMA) to be of benefit in improving vascular tone, blood flow, and vasoprotection [13, 14]. When administered to healthy subjects or to patients with visual disorders, VMA induced a significant improvement in night vision [10].

Correspondence: Professor Hideaki Hara, Department of Biofunctional Evaluation, Molecular Pharmacology, Gifu Pharmaceutical University, 5-6-1 Mitahora-higashi, Gifu 502-8585, Japan

E-mail: hidehara@gifu-pu.ac.jp

Fax: +81-58-237-8596

Abbreviations: CM-H₂DCFDA, 5-(and-6)-chloromethyl-2,7-dichlorodihydrofluorescein diacetate acetyl ester; GCL, ganglion cell layer; IC₅₀, 50% inhibitory concentration; IPL, inner plexiform layer; NMDA, *N*-methyl-D-aspartic acid; RGC, retinal ganglion cell; ROS, reactive oxygen species; SIN-1, 3-(4-morpholinyl) sydnonimine hydrochloride; TBARS, thiobarbituric acid reactive substance; TUNEL, terminal deoxynucleotidyl transferase-mediated dUTP nick-end labeling; VMA, *Vaccinium myrtillus* anthocyanoside

Hence, VMA has been utilized as a popular edible aid or supplement for asthenopia. However, the detailed mechanism(s) underlying improvements these in visual function remain unclear.

Free radical species, such as superoxide and nitric oxide, are associated with the pathogenesis of inflammatory diseases. Nitric oxide reacts with superoxide, forming peroxynitrite, which triggers cell death by apoptosis [15, 16]. Nitrotyrosine and lipid peroxide are produced when peroxynitrite reacts with tyrosine, proteins, and lipids under physiological conditions [17, 18], and high levels of lipid peroxide and nitrotyrosine induce RGC death [3, 4]. Previous studies have established that VMA has powerful antioxidant effects [8, 9, 12], and *via* such antioxidant effects VMA might be expected to protect the retina against oxidative stress. However, the effects of VMA and its main constituents (such as cyanidin, delphinidin, and malvidin) on peroxynitrite- and lipid peroxide-induced RGC death have not been investigated in *in vitro* or *in vivo* studies.

In previous *in vitro* studies, a high concentration of 3-(4-morpholinyl) sydnonimine hydrochloride (SIN-1) has been found to induce RGC-5 death [19], while *N*-methyl-D-aspartic acid (NMDA) receptor-mediated neurotoxicity has been reported to depend in part on the generation of nitric oxide and superoxide anions, which as mentioned above react to form peroxynitrite [15]. *In vivo*, intravitreal injection of NMDA reportedly induces RGC damage in the mouse retina, while the formation of superoxide, nitric oxide, and peroxynitrite plays a key role in NMDA-induced neurotoxicity in the rat retina [20, 21].

Against the above background, we designed the present study to examine the effects of VMA and its main constituents (cyanidin, delphinidin, and malvidin) on retinal damage both *in vitro* and *in vivo*. To this end, we studied its effects on: (i) SIN-1-induced neurotoxicity and radical activation in RGC cultures, (ii) lipid peroxidation in homogenates of mouse forebrain, and (iii) NMDA-induced retinal damage in mice *in vivo*.

2 Materials and methods

2.1 Materials

SIN-1 and 5-(and-6)-chloromethyl-2,7-dichlorodihydrofluorescein diacetate acetyl ester (CM-H₂DCFDA) were purchased from Dojindo (Kumamoto, Japan) and Invitrogen (Eugene, OR, USA), respectively, while NMDA was from Sigma–Aldrich (St. Louis, MO, USA). Cyanidin, delphinidin, and malvidin were purchased from Extrasynthese (Genay Cedex, France). VMA was kindly gifted by Fushimi Chemical (Kyoto, Japan).

2.2 HPLC analysis

A Waters 2695 series HPLC equipped with an UV/Visible detector at 520 nm was used with an RP C₁₈ column

(250 mm × 4.6 mm; Develosil ODS-HG-5; Nomura Chemical, Seto, Japan). The mobile phase was composed of 10% formic acid solution v/v (A) and formic acid/ACN/methanol/water (10:22.5:22.5:40 v/v) (B). The gradient was as follows: 0 min, 90% (A), 10% (B); 40 min, 65% (A), 35% (B). Elution was performed at a solvent flow rate of 1.0 mL/min. The column compartment was kept at a temperature of 25°C. VMA was dissolved in 10% formic acid solution (1 mg/mL), and the sample injection volume was 20 µL.

2.3 Animals

ddY Mice were obtained from Japan SLC (Hamamatsu, Japan). All mice were handled according to the ARVO statement for Use of Animals in Ophthalmic and Vision Research, and experiments were approved and monitored by the Institutional Animal Care and Use Committee of Gifu Pharmaceutical University.

2.4 RGC-5 culture

RGC-5 cells were kindly gifted by Dr. Neeraj Agarwal (UNT Health Science Center, Fort Worth, TX, USA). They were maintained in DMEM containing 10% fetal bovine serum (FBS), 100 U/mL penicillin (Meiji Seika Kaisha, Tokyo, Japan), and 100 µg/mL streptomycin (Meiji Seika) under a humidified atmosphere of 95% air and 5% CO₂ at 37°C. RGC-5 cells were passaged by trypsinization every 3–4 days, as described in our previous report [22].

2.5 Cell-survival assay

RGC-5 cells were seeded into a 96-well plate at a density 1000 cell/well at 37°C for 24 h, and preincubated in 1% FBS-DMEM with VMA or its main anthocyanidin constituents at 37°C for 1 h. After preincubation, SIN-1 (final concentration 0.5 mM) was added to these cultures for 23 h. The viable cell numbers were measured using a water-soluble tetrazolium salt, 2-(2-methoxy-4-nitrophenyl)-3-(4-nitrophenyl)-5-(2,4-disulphophenyl)-2H tetrazolium monosodium salt, in a WST-8 assay. Briefly, 10 µL of CCK-8 (Dojindo) was added to each well, incubated at 37°C for 4 h, and the absorbance measured at 492 nm (reference wave length, 660 nm) [23].

2.6 Measurement of radical activation in RGC-5

The intracellular radical activation within RGC-5 cells was determined using CM-H₂DCFDA. VMA and its main anthocyanidin constituents were pretreated for 1 h, and cells were then treated with CM-H₂DCFDA (final concentration 10 µM) for 15 min at 37°C. After 15 min, the medium was replaced with fresh medium containing the same compounds (except CM-H₂DCFDA). The 96-well plate was loaded into a plate-holder fluorescence spectro-

photometer (Varioskan®; Thermo Electron Corporation, Vantaa, Finland). The reaction was carried out at 37°C, and fluorescence was monitored at 488 nm excitation and 525 nm emission using the fluorescence spectrophotometer. After each well had been monitored as baseline for 30 s, the reaction was initiated by adding SIN-1 (final concentration 0.5 mM) from the autodispenser fitted to the equipment, and fluorescence was monitored for 10 min. Data were acquired and calculations made using Skanlt® Software for Varioskan ver.2.4.1 (Thermo Electron Corporation). Total intensity was calculated by integrating the area under the CM-H₂DCFDA fluorescence-intensity curve for 10 min after SIN-1 treatment [24].

2.7 Lipid peroxidation

The supernatant fraction of a forebrain homogenate from male adult ddY mice (body weight, 20–25 g) was prepared as previously described [25]. Briefly, brain tissues were homogenized in a glass-Teflon homogenizer in 4 vol of ice-cold phosphate-saline buffer (50 mM, pH 7.4), and the homogenate was stored at –80°C. This stock brain homogenate was diluted ten-fold with the same buffer. Then, 1 mL portions of the diluted homogenate were added to 5 µL of the test compounds, and incubated at 37°C for 30 min. The reaction was stopped by adding 200 µL of 35% HClO₄, followed by centrifugation at 2800 rpm for 10 min. The supernatant (500 µL) was heated with 250 µL of thiobarbituric acid (TBA) solution (5 g/L in 50% acetic acid) for 15 min at 100°C. Absorbance was then measured at 532 nm. We calculated the 50% inhibitory concentration (IC₅₀) of the thiobarbituric acid reactive substance (TBARS).

2.8 NMDA-induced retinal damage

Male adult ddY mice weighing 37–43 g were kept under lighting conditions involving 12 h light and 12 h dark. Anesthesia was induced with 3.0% isoflurane and maintained with 1.5% isoflurane in 70% N₂O and 30% O₂ via an animal general anesthesia machine (Soft Lander; Sin-ei Industry, Saitama, Japan). Retinal damage was induced by the injection (2 µL *per eye*) of NMDA dissolved at 2.5 mM in saline. This was injected into the vitreous body of the left eye under the above anesthesia. One drop of levofloxacin ophthalmic solution (Santen Pharmaceuticals, Osaka, Japan) was applied topically to the treated eye immediately after the intravitreal injection. Seven days (for hematoxylin and eosin staining) or 24 h (for terminal deoxynucleotidyl transferase-mediated dUTP nick-end labeling (TUNEL) staining) after the NMDA injection, eye balls were enucleated for histological analysis. VMA at 10 or 100 µg *per eye* was dissolved in saline and co-administered with the NMDA.

2.9 Histological analysis: Hematoxylin and eosin staining

In mice under anesthesia produced by an intraperitoneal injection of sodium pentobarbital (Dainippon Sumitomo Pharma, Osaka, Japan) at 80 mg/kg, each eye was enucleated and kept immersed for at least 24 h at 4°C in a fixative solution containing 4% paraformaldehyde. Six paraffin-embedded sections (thickness 5 µm) cut through the optic disk of each eye were prepared in a standard manner and stained with hematoxylin and eosin. Retinal damage was evaluated as described previously [26], three sections from each eye being used for the morphometric analysis. Light-microscope images were photographed, and (i) the cell counts in the ganglion cell layer (GCL) at a distance between 375 and 625 µm from the optic disk and (ii) the thickness of the inner plexiform layer (IPL) were measured on the photographs in a masked fashion by a single observer. Data from three sections (selected randomly from the six sections) were averaged for each eye, and used to evaluate the cell count in the GCL and the thickness of the IPL.

2.10 TUNEL staining

In mice under anesthesia produced by an intraperitoneal injection of sodium pentobarbital at 80 mg/kg, each eye was enucleated, fixed in 4% paraformaldehyde overnight at 4°C, immersed in 20% sucrose for 48 h at 4°C, and embedded in optimum cutting temperature (OCT) compound (Sakura Finetechnical, Tokyo, Japan). Cryostat sections (10 µm thick) were cut and placed on slides (Mass Coat). TUNEL staining was performed according to the manufacturer's instructions (Roche Molecular Biochemical, Mannheim, Germany). By immersion, sections were reacted with 3% H₂O₂ in methanol for 10 min at room temperature and then washed after which 0.1% ferric sodium in citrate plus 0.1% Triton X-100 (BioRad laboratories, Hercules, CA, USA) solution was added and the sections were incubated for 2 min on ice. After immersion, sections were incubated in a terminal deoxynucleotidyl transferase (TdT) labeling reaction mixture (supplied with the kit) in a humidified chamber for 1 h at 37°C. To quantify DNA-fragmented cells after injection of NMDA, light-microscope images were photographed, and the numbers of TUNEL-positive cells were counted in GCL at a distance between 375 and 805 µm from the optic disk in a masked fashion by a single observer (NM).

2.11 Statistical analysis

Data are presented as mean ± SEM. Statistical comparisons were made using a one-way analysis of variance (ANOVA) followed by a student's *t*-test or Dunnett's multiple-compar-

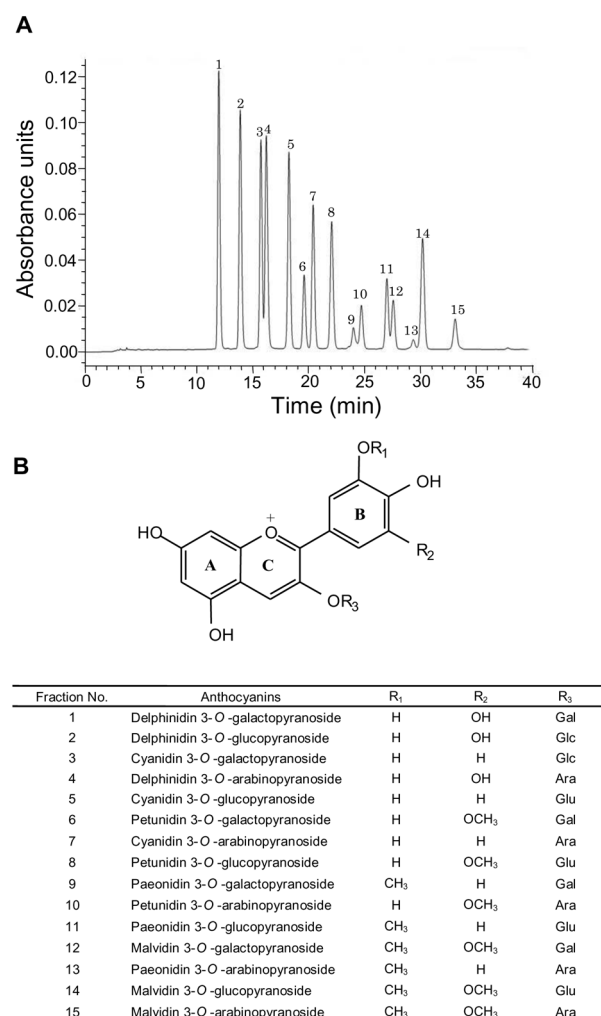


Figure 1. HPLC separation of VMA, A: use of 520 nm as a selective wavelength allowed identification of 15 anthocyanosides. The various peak numbers correspond to the “Fraction No.” in (B). B: Chemical structure of VMA. Anthocyanidins, a subclass of flavonoids, are defined by their three-ring (C₆C₃C₆) structure consisting of two benzene rings (A and B rings) flanking an oxygen-containing pyran ring (C ring). VMA contains five anthocyanidins, and each of these can be linked to a different saccharide, which may be glucose, galactose, or arabinose; hence there are 15 different compounds. Cyanidin and delphinidin are representative hydroxyflavones and malvidin a representative methoxyflavone in VMA. Glc, glucose; Gal, galactose; Ara, arabinose.

ison test. A value of $p < 0.05$ was considered to indicate statistical significance.

3 Results

3.1 HPLC analysis

Fifteen anthocyanin components of VMA were confirmed by HPLC analysis (Fig. 1A), and these are listed in Fig. 1B.

Our HPLC data were almost same as previous studies [7, 8] (Fig. 1). We selected three anthocyanidins: cyanidin (cyanidin 3-O-galactopyranoside, cyanidin 3-O-glucopyranoside, and cyanidin 3-O-arabinopyranoside), delphinidin (delphinidin 3-O-galactopyranoside, delphinidin 3-O-glucopyranoside, and delphinidin 3-O-arabinopyranoside) and malvidin (malvidin 3-O-galactopyranoside, malvidin 3-O-glucopyranoside, and malvidin 3-O-arabinopyranoside) from VMA.

3.2 SIN-1-induced RGC-5 cell death

Our previous study indicated that VMA at 10 $\mu\text{g/mL}$ inhibits VEGF-induced angiogenesis (inhibition of tube formation, proliferation, and migration), by inhibiting both the cell proliferation and migration induced by VEGF [12]. VMA at 10 $\mu\text{g/mL}$ contains cyanidin at 2.6 μM , delphinidin at 4.5 μM , and malvidin at 1.4 μM (calculated as anthocyanidin based on [7]), and these concentrations of VMA and anthocyanidin can be expected to have pharmacological effects. On the basis of these findings, we used VMA at concentrations of 1–10 $\mu\text{g/mL}$ and anthocyanidins at 1–30 μM in the present *in vitro* studies. SIN-1 induced death in approximately 40% of RGC-5, and VMA at 10 $\mu\text{g/mL}$ significantly inhibited this SIN-1-induced RGC-5 cell death (~90% of cells remaining viable) (Fig. 2A). Cyanidin at 10 μM , delphinidin at 30 μM , and malvidin at 10 μM significantly inhibited the SIN-1-induced cell death (~75% of cells viable) (Figs. 2B–D). At these concentrations, VMA, cyanidin, delphinidin, or malvidin alone had no effects on the viability of RGC-5 (Figs. 2A–D).

3.3 SIN-1-induced radical elevation in RGC-5 cells

CM-H₂DCFDA, a cell-permeant indicator of reactive oxygen species (ROS), is nonfluorescent until removal of its acetate groups by intracellular esterase. Within the cell, esterases cleave CM-H₂DCFDA to release CM-H₂DCFH, which is converted to a fluorescent product (CM-H₂DCF) when exposed to ROS. VMA at 10 $\mu\text{g/mL}$, cyanidin at 3.0–30 μM , delphinidin at 10 and 30 μM , and malvidin at 10 and 30 μM all significantly inhibited the SIN-1-induced radical activity in RGC-5 cells (Fig. 3), decreasing intracellular radical formation by 71%, 25–81%, 34–51%, and 57–78%, respectively (Fig. 3).

3.4 Lipid peroxidation in mouse forebrain homogenates

In the lipid peroxidation study, the TBARS level in mouse forebrain homogenate was elevated increased after 30 min incubation at 37°C. VMA, cyanidin, delphinidin, and malvidin each inhibited the production of TBARS in a concentration-dependent manner, the IC₅₀ values being 1.0 $\mu\text{g/mL}$, 0.7, 1.9, and 8.3 μM , respectively (Table 1).

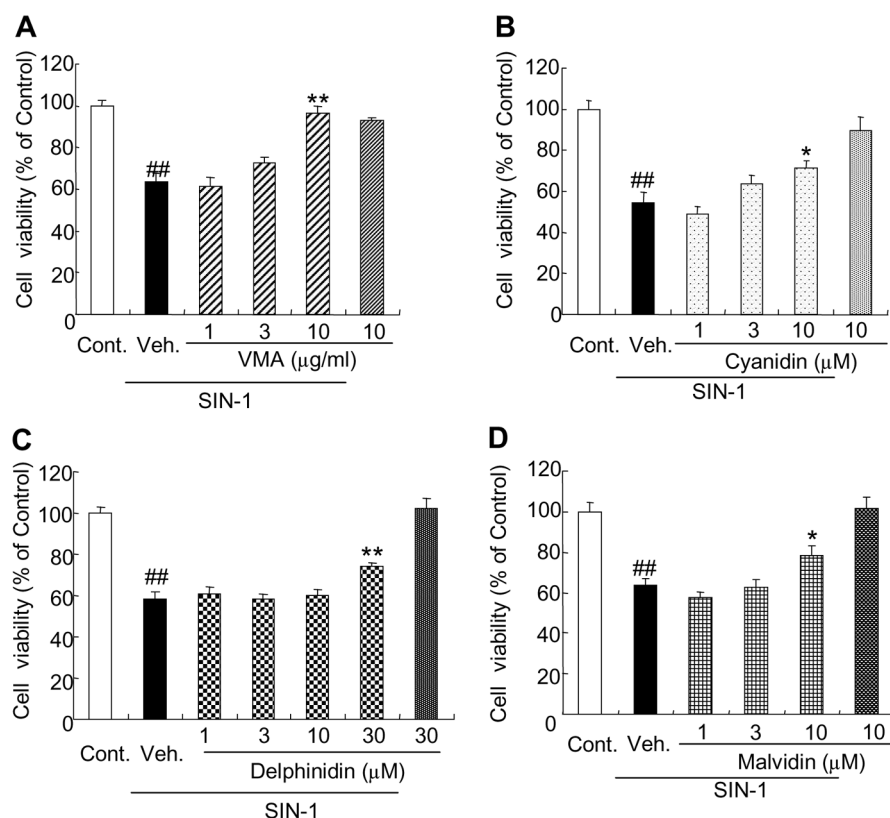


Figure 2. Effects of VMA and anthocyanidins (cyanidin, delphinidin, and malvidin) on SIN-1-induced RGC-5 death. RGC-5 were cultured in 96-well plates at a density of 1000 cells/well, then incubated for a total of 48 h at 37°C in 5% CO₂. Cell viability was assessed by immersing cells in CCK-8 for 4 h at 37°C, with photometric data being recorded at 492/660 nm. A, B, C, and D: Effects of VMA, cyanidin, delphinidin, and malvidin on SIN-1-induced RGC-5 death. The last bars in each figure (A–D) are shown data of the application of each drug alone. Data are shown as mean ± SEM ($n = 5$ or 6). Cont., control; Veh., vehicle. ##, $p < 0.01$ versus control, and *, $p < 0.05$, **, $p < 0.01$ versus vehicle.

Table 1. The IC₅₀ values for effects of VMA and anthocyanidins (cyanidin, delphinidin, and malvidin) on lipid peroxidation in mouse forebrain homogenates

Compounds	TBARS IC ₅₀	95% Confidence limits
VMA	1.0 µg/mL	0.8–1.4
Cyanidin	0.7 µM	0.4–1.0
Delphinidin	1.9 µM	1.4–2.4
Malvidin	8.3 µM	5.7–20.2

3.5 Retinal damage induced by intravitreal injection of NMDA in mice

Intravitreal injection of NMDA at 5 nmol *per eye* significantly decreased both the cell count in GCL and the thickness of IPL in the mouse retina. The GCL cell counts in control mice and NMDA-injected mice were 124.4 ± 2.9 (mean ± SEM, $n = 6$) and 66.5 ± 5.5 ($n = 11$), respectively (Fig. 4B). The values obtained for IPL thickness in control mice and NMDA-injected mice were 39.7 ± 2.0 ($n = 6$) µm and 27.5 ± 2.0 ($n = 11$) µm, respectively (Fig. 4C). Intravitreal injection of VMA at 100 µg *per eye* (co-injected with

NMDA at 5 nmol *per eye*) significantly inhibited this retinal damage (both the GCL cell count and the IPL thickness), but VMA at 10 µg *per eye* did not (Fig. 4). The GCL cell counts in NMDA-injected mice and NMDA plus VMA (100 µg *per eye*)-injected mice were 66.5 ± 5.5 ($n = 11$) and 86.8 ± 4.4 ($n = 9$), respectively (Fig. 4B). The values obtained for IPL thicknesses in NMDA-injected mice and NMDA plus VMA (100 µg *per eye*)-injected mice were 27.5 ± 2.0 ($n = 11$) µm and 35.8 ± 2.2 ($n = 9$) µm, respectively (Fig. 4C).

3.6 Apoptosis induced in GCL cells by intravitreal injection of NMDA in mice

We examined the effects of VMA on NMDA-induced apoptosis in mouse GCL using TUNEL staining. Intravitreal injection of NMDA at 5 nmol *per eye* significantly increased TUNEL-positive cells in GCL, the TUNEL-positive cell-counts in GCL in control mice and NMDA-injected mice being 4.6 ± 0.9 (mean ± SEM, $n = 11$) and 41.5 ± 1.3 ($n = 9$), respectively (Fig. 5B). Intravitreal injection of VMA at 100 µg *per eye* (co-injected with

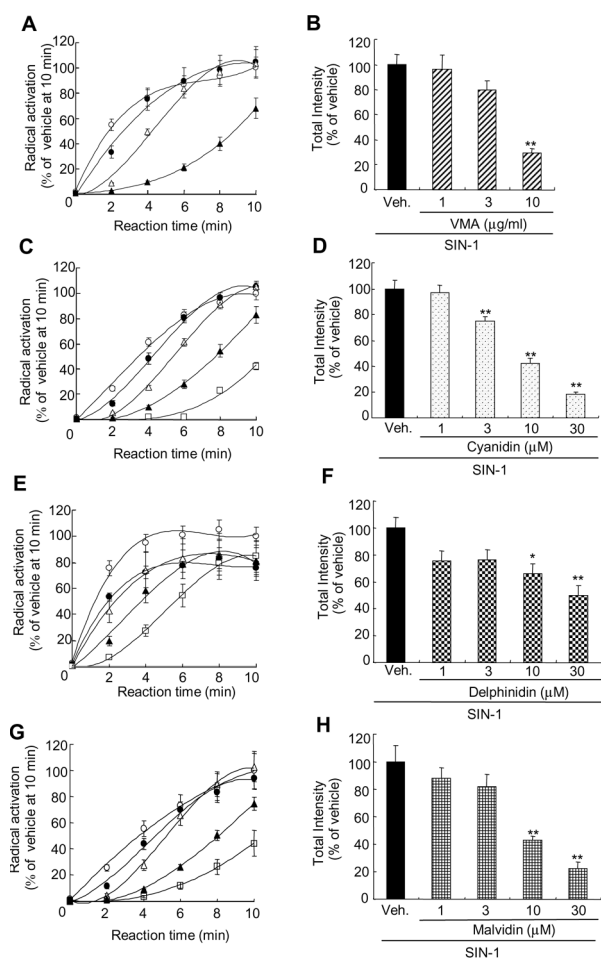


Figure 3. Effects of VMA and anthocyanidins (cyanidin, delphinidin, and malvidin) on SIN-1-induced production of ROS. Intracellular ROS levels were determined by measuring the fluorescence of CM-H₂DCFDA (at excitation 488 nm *per* emission 525 nm) every 2 min for a total of 10 min. A, C, E, and G: effects of VMA, cyanidin, delphinidin, and malvidin, respectively, on time-dependent SIN-1-induced intracellular radical activation. A: Vehicle, and SIN-1 plus VMA at 1.0, 3.0, or 10 μg/mL are shown as open circle, closed circle, open triangle, and closed triangle, respectively. C, E, and G: Vehicle, and SIN-1 plus a given anthocyanidin at 1, 3, 10, and 30 μM are shown as open circle, closed circle, open triangle, and open box, respectively. B, D, F, and H: Data in A, C, E, and G were used to calculate total intensity (as described in Section 2). Data are shown as mean ± SEM (*n* = 5 or 6). Veh., vehicle. *, *p* < 0.05, **, *p* < 0.01 *versus* vehicle.

NMDA at 5 nmol *per* eye) significantly decreased this effect, the TUNEL-positive cell-count in GCL following intravitreal injection of NMDA plus VMA being 31.6 ± 1.3 (*n* = 10) (Fig. 5B).

4 Discussion

In the present study, we found that VMA and its main anthocyanidin constituents (cyanidin, delphinidin, and malvidin)

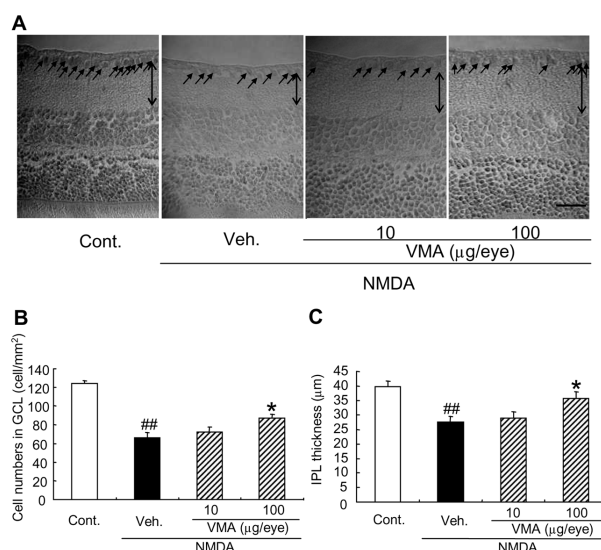


Figure 4. Effect of VMA on NMDA-induced retinal damage in mice. Hematoxylin and eosin staining of sections (thickness 5 μm) obtained from mice at 7 days after intravitreal injection of NMDA. A: Representative photographs show non-treated control retina, NMDA-injected vehicle-treated retina, retina treated with NMDA-injection plus VMA at 10 μg *per* eye, and retina treated with NMDA-injection plus VMA at 100 μg *per* eye. Horizontal bar represents 25 μm. Vertical bar and arrows indicate IPL and RGC, respectively. B and C: Cell numbers in RGC and thickness of IPL. Data are shown as mean ± SEM (*n* = 6–11). Cont., control; Veh., vehicle. ##, *p* < 0.01 *versus* control, and *, *p* < 0.05 *versus* vehicle.

all protected RGC-5 cells against SIN-1-induced cell death *in vitro*. In our *in vivo* study, intravitreal injection of VMA inhibited NMDA-induced retinal damage in mice. Further, VMA and all three of these anthocyanidins inhibited the SIN-1-induced elevation of ROS in RGC-5.

VMA contains 15 kinds of anthocyanins [7, 8], a finding we confirmed using HPLC analysis. Actually, VMA contains five anthocyanidins (cyanidin, delphinidin, petunidin, paeonidin, and malvidin), and each of these can be linked to a different saccharide, which may be glucose, galactose, or arabinose. The delphinidin and cyanidin contents of VMA are higher than those of the other anthocyanidins [7, 8]. Further, anthocyanins containing delphinidin exhibit higher absorption ratios than the other anthocyanins in VMA [27]. The availability of the hydroxyl group on the B ring (benzene ring on right side of structure in Fig. 1B) of an anthocyanidin (*e.g.*, cyanidin and delphinidin) is fundamental to the antioxidant activity of these compounds because these hydroxyl moieties can donate hydrogen to scavenge radicals [28, 29]. Indeed, the donated hydrogen serves to scavenge oxygen radicals such as superoxide and hydroxyl radicals [29]. Moreover, the donation of hydrogen to peroxy radical can break the chain reactions involved in lipid peroxidation [29]. Previous studies have reported that malvidin-glucopyranoside inhibits the free radical-initiated per-

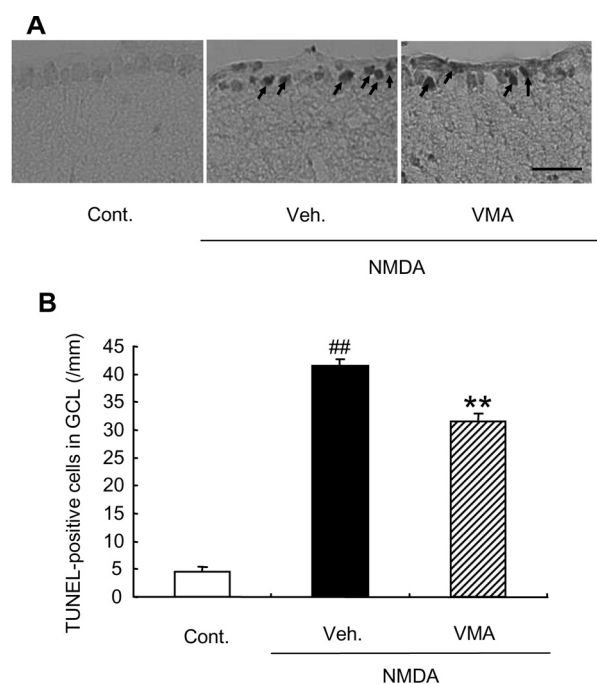


Figure 5. Effects of VMA on NMDA-induced increase in number TUNEL-positive cells. (A) Representative photographs show non-treated control retina, NMDA-injected vehicle-treated retina, and retina treated with NMDA-injection plus VMA at 100 µg per eye. Arrows show TUNEL-positive cells. Horizontal bar represents 25 µm. (B) TUNEL-positive cell numbers in RGC. Data are shown as mean ± SEM ($n = 9–11$). Cont., control; Veh., vehicle. ##, $p < 0.01$ versus control, and **, $p < 0.01$ versus vehicle.

oxidation of linoleic acid [30, 31]. In the present study, VMA and its main constituents all inhibited lipid peroxidation in mouse forebrain homogenates. Taken together, these findings indicate that VMA and its main constituents (cyanidin, delphinidin, and malvidin) have antioxidant effects.

Our previous study indicated that VMA at 10 µg/mL inhibits VEGF-induced angiogenesis (inhibition of tube formation, proliferation, and migration), by inhibiting both the cell proliferation and migration induced by VEGF [12]. VMA at 10 µg/mL contains cyanidin at 2.6 µM, delphinidin at 4.5 µM, and malvidin at 1.4 µM (calculated as anthocyanidin) [7], and these concentrations of VMA and anthocyanidin can be expected to have pharmacological effects. On the basis of these findings, we used VMA at concentrations of 1 to 10 µg/mL and anthocyanidins at 1 to 30 µM in the present *in vitro* studies.

Bao *et al.* have reported that oral administration of anthocyanin at 84 mg/kg (200 mg/kg bilberry extract) significantly decreased malondialdehyde and nitric oxide level in the mouse liver. Further, they suggested that bilberry extract plays an important role in protecting against restraint stress-induced liver damage by both scavenging free radicals activity and lipid peroxidation inhibitory effect [32]. In

addition, Morazzoni *et al.* [33] have reported that absolute bioavailability by oral administration of VMA is 1.2%. Taken together, if anthocyanins at 84 mg/kg are administered by oral route, the bioavailability is 40.3 µg. For that reason, we performed intravitreal injection of VMA at 10–100 µg per eye (anthocyanin at 3.6–36 µg per eye (since VMA contain 36% anthocyanin)).

Trackey *et al.* [34] noted that addition of SIN-1 to mouse cortical cell cultures increases the release of cellular proteins containing nitrotyrosine into the cell-culture medium, and that this phenomenon occurs in parallel with cortical cell injury. They therefore considered that SIN-1 induces neurotoxicity through an intracellular elevation of peroxynitrite [34]. In addition, SIN-1 has been described as a peroxynitrite donor because it produces both nitric oxide and superoxide upon decomposition in aqueous solution and in biological tissues [34–36]. We decided to examine the effect of VMA and anthocyanidins (cyanidin, delphinidin, and malvidin) on SIN-1-induced RGC-5 death *in vitro*, a subject that had not been investigated before despite previous studies reporting that peroxynitrite induces lipid peroxidation and that the lipoperoxide induces RGC-5 death [4, 17, 37]. In the present study, VMA, cyanidin, delphinidin, and malvidin inhibited lipid peroxidation in mouse forebrain homogenates, each in a concentration-dependent manner. Notably, cyanidin inhibited lipid peroxidation more powerfully than delphinidin and malvidin (Table 1). Moreover: (i) the inhibitory effect of cyanidin on the SIN-1-induced elevation of ROS was stronger than that of delphinidin and at least as strong as that of malvidin (Fig. 3), and (ii) cyanidin and malvidin inhibited SIN-1-induced RGC death more powerfully than delphinidin (Fig. 2). Therefore, among these anthocyanidins, cyanidin may play the most important role in the neuroprotective effect of VMA against SIN-1-induced oxidative stress-related damage described in the present study.

The neurotoxicity associated with overstimulation of NMDA receptors is thought to be mediated by an excessive calcium-ion influx. A phenomenon leading to a series of potentially neurotoxic events [38]. One of these events is activation of nitric oxide synthase and the subsequent production of nitric oxide [39]. Another event is stimulation of phospholipase A₂ or calcium-ion overload in mitochondria, leading to the generation of superoxide anion [40]. Nitric oxide reacts with superoxide anion to form peroxynitrite [41], which results in neuronal damage [42]. El-Remessy *et al.* [21] demonstrated not only that NMDA-induced retinal neurotoxicity is closely related to the formation of nitrite, nitrotyrosine, and lipid peroxidation, but also that intravitreal injection of N^G-nitro-L-arginine methyl ester hydrochloride (L-NAME, a nitric oxide synthase inhibitor) inhibited NMDA-induced neurotoxicity in the rat retina (based on a TUNEL assay) [21]. In the present study, we found that VMA protected retinal neurons against NMDA-induced damage in mice (Fig. 4), and that it inhibited the NMDA-

induced increase in TUNEL-positive cells (apoptotic cells) in the retina (Fig. 5). In our study, we noted that L-NAME significantly inhibited the NMDA (5 nmol *per eye*)-induced increase in TUNEL-positive cells in the mouse retina (unpublished data, Matsunaga *et al.*). This is the first report demonstrating that in the VMA can protect the retina against NMDA-induced neurotoxicity *in vivo*. Furthermore, we found that VMA was effective against the SIN-1-induced elevation of ROS and against lipid peroxidation in mouse forebrain homogenates. Taken together, the above findings indicate that the protective effects of VMA against NMDA-induced neurotoxicity may be partly mediated by an inhibition of NMDA-induced oxidative stress.

In conclusion, VMA and its main anthocyanidin constituents (cyanidin, delphinidin, and malvidin) inhibited SIN-1-induced RGC-5 death *in vitro*, and these neuroprotective effects may be mediated by inhibition of oxidative stress. In addition, VMA exhibited neuroprotective effects against NMDA-induced retinal damage in mice *in vivo*. These findings indicate that VMA may have potential as an agent to be used to retard or prevent retinal degenerative diseases such as glaucoma.

We thank Mr. Kazuo Kasemura for useful advice and technical support (HPLC data).

The authors have declared no conflict interest.

5 References

- [1] Bonne, C., Muller, A., Villain, M., Free radicals in retinal ischemia. *Gen. Pharmacol.* 1998, 30, 275–280.
- [2] Dreyer, E. B., A proposed role for excitotoxicity in glaucoma. *J. Glaucoma* 1998, 7, 62–67.
- [3] Neufeld, A. H., Nitric oxide: A potential mediator of retinal ganglion cell damage in glaucoma. *Surv. Ophthalmol.* 1999, 43, S129–S135.
- [4] Levin, L. A., Clark, J. A., Johns, L. K., Effect of lipid peroxidation inhibition on retinal ganglion cell death. *Invest. Ophthalmol. Vis. Sci.* 1996, 37, 2744–2749.
- [5] McKinnon, S. J., Glaucoma, apoptosis, and neuroprotection. *Curr. Opin. Ophthalmol.* 1997, 8, 28–37.
- [6] Shimazawa, M., Inokuchi, Y., Ito, Y., Murata, H. *et al.*, Involvement of ER stress in retinal cell death. *Mol. Vis.* 2007, 13, 578–587.
- [7] Baj, A., Bombardelli, E., Gabetta, A., Martinelli, E. M., Qualitative and quantitative evaluation of Vaccinium myrtillus anthocyanins by high resolution gas chromatography and high performance liquid chromatography. *J. Chromatogr.* 1983, 279, 365–372.
- [8] Nakajima, J., Tanaka, I., Seo, S., Yamazaki, M., Saito, K., LC/PDA/ESI-MS profiling and radical scavenging activity of anthocyanins in various berries. *J. Biomed. Biotechnol.* 2004, 2004, 241–247.
- [9] Zafra-Stone, S., Yasmin, T., Bagchi, M., Chatterjee, A. *et al.*, Berry anthocyanins as novel antioxidants in human health and disease prevention. *Mol. Nutr. Food Res.* 2007, 51, 675–683.
- [10] Morazzoni, P., Bombardelli, E., Vaccinium myrtillus. *Fytoterapia* 1996, 67, 3–29.
- [11] Morazzoni, P., Magistretti, M. J., Activity of Myrtocyan®, an anthocyanoside complex from Vaccinium myrtillus (VMA), on platelet aggregation and adhesiveness. *Fytoterapia* 1990, 61, 13–21.
- [12] Matsunaga, N., Chikaraisi, Y., Shimazawa, M., Yokota, S., Hara, H., Vaccinium myrtillus (Bilberry) extracts reduce angiogenesis *in vitro* and *in vivo*. *eCAM* 2007, 20, DOI:10.1093/ecam/nem151.
- [13] Lietti, A., Cristoni, A., Picci, M., Studies on Vaccinium myrtillus anthocyanosides. I. Vasoprotective and antiinflammatory activity. *Arzneimittelforschung* 1976, 26, 829–832.
- [14] Colantuoni, A., Bertuglia, S., Magistretti, M. J., Donato, L., Effects of Vaccinium myrtillus anthocyanosides on arterial vasomotion. *Arzneimittelforschung* 1991, 41, 905–909.
- [15] Bonfoco, E., Krainc, D., Ankarcrona, M., Nicotera, P., Lipton, S. A., Apoptosis and necrosis: Two distinct events induced, respectively, by mild and intense insults with N-methyl-D-aspartate or nitric oxide/superoxide in cortical cell cultures. *Proc. Natl. Acad. Sci. U. S. A.* 1995, 92, 7162–7166.
- [16] Miles, A. M., Bohle, D. S., Glassbrenner, P. A., Hansert, B. *et al.*, Modulation of superoxide-dependent oxidation and hydroxylation reactions by nitric oxide. *J. Biol. Chem.* 1996, 271, 40–47.
- [17] Radi, R., Beckman, J. S., Bush, K. M., Freeman, B. A., Peroxynitrite-induced membrane lipid peroxidation: the cytotoxic potential of superoxide and nitric oxide. *Arch. Biochem. Biophys.* 1991, 288, 481–487.
- [18] Eiserich, J. P., Hristova, M., Cross, C. E., Jones, A. D. *et al.*, Formation of nitric oxide-derived inflammatory oxidants by myeloperoxidase in neutrophils. *Nature* 1998, 391, 393–397.
- [19] Eissa, L. A., Smith, S. B., El-Sherbeny, A., Regulation of taurine transporter activity in cultured rat retinal ganglion cells and rat retinal Müller cells. *Saudi Pharm. J.* 2006, 14, 16–26.
- [20] Li, Y., Schlamp, C. L., Nickells, R. W., Experimental induction of retinal ganglion cell death in adult mice. *Invest. Ophthalmol. Vis. Sci.* 1999, 40, 1004–1008.
- [21] El-Remessy, A. B., Khalil, I. E., Matragoon, S., Abou-Mohamed, G. *et al.*, Neuroprotective effect of (–) delta9-tetrahydrocannabinol and cannabidiol in N-methyl-D-aspartate-induced retinal neurotoxicity: Involvement of peroxynitrite. *Am. J. Pathol.* 2003, 163, 1997–2008.
- [22] Shimazawa, M., Yamashita, T., Afarwal, N., Hara, H., Neuroprotective effects of minocycline against *in vitro* and *in vivo* retinal cell damage. *Brain Res.* 2005, 1053, 185–194.
- [23] Tominaga, H., Ishiyama, M., Ohseto, F., Sasamoto, K. *et al.*, A water-soluble tetrazolium salt useful for colorimetric cell viability assay. *Anal. Commun.* 1999, 36, 47–50.
- [24] Nakajima, Y., Inokuchi, Y., Shimazawa, M., Otsubo, K. *et al.*, Astaxanthin, a dietary carotenoid, protects retinal cells against oxidative stress *in vitro* and *in vivo*. *J. Pharm. Pharmacol.* 2008, 60, 1365–1374.
- [25] Hara, H., Kogure, K., Prevention of hippocampus neuronal damage in ischemic gerbils by a novel lipid peroxidation inhibitor (quinazoline derivative). *J. Pharmacol. Exp. Ther.* 1990, 255, 906–913.

- [26] Yoneda, S., Tanihara, H., Kido, N., Honda, Y. *et al.*, Interleukin-1 β mediates ischemic injury in the rat retina. *Exp. Eye Res.* 2001, 73, 661–667.
- [27] Talav era, S., Felgines, C., Texier, O., Besson, C. *et al.*, Anthocyanins are efficiently absorbed from the stomach in anesthetized rats. *J. Nutr.* 2003, 133, 4178–4182.
- [28] Vinson, J. A., Dabbagh, Y. A., Serry, M. M., Jang, J., Plant flavonoids, especially tea flavonols, are powerful antioxidants using an in vitro oxidation model for heart disease. *J. Agric. Food Chem.* 1995, 43, 2800–2802.
- [29] Torel, J., Cillard, J., Cillard, P., Antioxidant activity of flavonoids and reactivity with peroxy radical. *Phytochemistry* 1986, 25, 383–385.
- [30] Rossetto, M., Vanzani, P., Mattivi, F., Lunelli, M. *et al.*, Synergistic antioxidant effect of catechin and malvidin 3-glucoside on free radical-initiated peroxidation of linoleic acid in micelles. *Arch. Biochem. Biophys.* 2002, 408, 239–245.
- [31] Tamura, H., Yamagami, A., Antioxidative activity of monoacylated anthocyanins isolated from Muscat Bailey a grape. *J. Agric. Food Chem.* 1994, 42, 1612–1615.
- [32] Bao, L., Yao, X. S., Yau, C. C., Tsi, D. *et al.*, Protective effects of bilberry (*Vaccinium myrtillus* L.) extract on restraint stress-induced liver damage in mice. *J. Agric. Food. Chem.* 2008, 56, 7803–7807.
- [33] Morazzoni, P., Livio, S., Scilingo, A., Malandrino, S., *Vaccinium myrtillus* anthocyanosides pharmacokinetics in rats. *Arzneimittelforschung* 1991, 41, 128–131.
- [34] Trackey, J. L., Uliasz, T. F., Hewett, S. J., SIN-1-induced cytotoxicity in mixed cortical cell culture: Peroxynitrite-dependent and -independent induction of excitotoxic cell death. *J. Neurochem.* 2001, 79, 445–455.
- [35] Feelisch, M., The biochemical pathways of nitric oxide formation from nitrovasodilators: Appropriate choice of exogenous NO donors and aspects of preparation and handling of aqueous NO solutions. *J. Cardiovasc. Pharmacol.* 1991, 17, S25–S33.
- [36] Holm, P., Kankaanranta, H., Mets a-Ketela, T., Moilanen, E., Radical releasing properties of nitric oxide donors GEA 3162, SIN-1 and S-nitroso-N-acetylpenicillamine. *Eur. J. Pharmacol.* 1998, 346, 97–102.
- [37] Darley-Usmar, V. M., Hogg, N., O'Leary, V. J., Wilson, M. T., Moncada, S., The simultaneous generation of superoxide and nitric oxide can initiate lipid peroxidation in human low density lipoprotein. *Free Radic. Res. Commun.* 1992, 17, 9–20.
- [38] Lipton, S. A., Rosenberg, P. A., Excitatory amino acids as a final common pathway for neurologic disorders. *N. Engl. J. Med.* 1994, 330, 613–622.
- [39] Dawson, V. L., Dawson, T. M., London, E. D., Bredt, D. S., Snyder, S. H., Nitric oxide mediates glutamate neurotoxicity in primary cortical cultures. *Proc. Natl. Acad. Sci. U. S. A.* 1991, 88, 6368–6371.
- [40] Lafon-Cazal, M., Pietri, S., Culcasi, M., Bockaert, J., NMDA-dependent superoxide production and neurotoxicity. *Nature* 1993, 364, 535–537.
- [41] Beckman, J. S., Beckman, T. W., Chen, J., Marshall, P. A., Freeman, B. A., Apparent hydroxyl radical production by peroxynitrite: Implications for endothelial injury from nitric oxide and superoxide. *Proc. Natl. Acad. Sci. U. S. A.* 1990, 87, 1620–1624.
- [42] Lipton, S. A., Choi, Y. B., Pan, Z. H., Lei, S. Z. *et al.*, A redox-based mechanism for the neuroprotective and neurodestructive effects of nitric oxide and related nitroso-compounds. *Nature* 1993, 364, 626–632.